NONISOTHERMAL FLOW IN DOUBLY CONNECTED DOMAINS WITH POROUS BOUNDARIES

D. D. Aksenenko, G. H. Nesterov, and F. F. Spiridonov

UDC 532.516

The well-known vorticity–stream function approach [1], which is often used to calculate flows in doubly connected domains with imporous walls, is applied here to a case including injection and suction of gas through porous walls. The injection and suction of gas substantially complicate the problem as the stream function varies and is often undetermined. The proposed method allows one to overcome the difficulties that arise while formulating and solving this problem.

1. Consider a parallel and axisymmetric flow of a viscous diathermal gas in the doubly connected domain D, bounded by the contours S (abcdghpq) and L (kℓmn) (Fig. 1). The gas is injected through the porous segments ℓm and nk of the contour L, while it exits the domain D through the section qa of the contour S.

The flow is described by the following system of equations:

$$(\nabla, \nabla)\Psi = -\Omega, \quad \mathrm{Re}(\mathbf{W}, \nabla)\Omega = (\nabla, \nabla)\Omega + \nu\frac{\partial}{\partial Y}\left(\frac{\Omega}{Y}\right), \tag{1.1}$$

$$\mathrm{Pe}(\mathbf{W}, \nabla)\Theta = (\nabla, \nabla)\Theta + \nu\frac{\partial\Theta}{\partial Y},$$

where Re and Pe are the Reynolds and Peclet numbers respectively, W is the velocity vector with components u and v (Fig. 1), Θ is the temperature, ∇ is the gradient operator, $(\nabla, \nabla) = \partial^2/\partial Z^2 + \partial^2/\partial Y^2$ is the Laplace operator, (W, ∇) is the convective derivative, $\omega = -[\partial/\partial y(1/y^\nu\rho\cdot\partial\Psi/\partial y + \partial/\partial z(1/y^\nu\rho\cdot\partial\Psi/\partial z)]$ is the vorticity, $\partial\Psi/\partial y = y^\nu\rho u$ and $\partial\Psi/\partial z = -y^\nu\rho v$ are the derivatives of the stream function, ρ is the gas density, and ν is defined as $\nu = \begin{cases} 0, & \text{for parallel flow,} \\ 1, & \text{for axisymmetric flow.} \end{cases}$ All nondimensional quantities are denoted by the upper-case letters, and all dimensional ones by the lower-case letters. It is assumed that the heat loss due to viscous dissipation is negligibly small.

Following [2], the system of equations (1.1) reduces to an algebraic system of finite difference equations which is solved by the iterative method of successive relaxation with the Chebyshev polynomial parameters for Ψ. The convergence criterion uses the maximum relative discrepancy for all the variables. The dependence of the gas density on the temperature was determined by the equation of state for an ideal gas at constant pressure $\rho = \rho_0(\theta/\theta_0)$, where θ_0 is the temperature of the injected gas.

2. The boundary conditions for the temperature were altered within the range of $\theta_w = \theta_w/\theta_0$ between 0.13 and 1, and for $\theta_t = \theta_t/\theta_0$ between 0.36 and 1, where the subscript w denotes the temperature in the segments bc, cd, and dg of the contour S, and the subscript t the temperature in the segments ℓk and mn of the contour L. The temperature boundary conditions for the axis of symmetry gq, the outlet *qa*, and the segments ℓm and nk of the contour L are $\partial\theta/\partial y = 0$, $\partial\theta/\partial z = 0$, and $\theta = \theta_0$, respectively.

The boundary conditions for the vorticity were posed as recommended in [3]. In order to overcome the difficulties caused by posing the boundary conditions for the stream function (e.g., to eliminate the nonuniqueness of Ψ on the contour L), the original doubly connected domain D is replaced by the simply connected domain D_1, bounded by the contour G (abcdghkℓmnopq). This was accomplished by introducing the fictitious boundaries hk and op. It is assumed that the gas parameters are identical on both fictitious boundaries. In order to minimize the geometrical distortion of the computational domain under consideration, the distance between fictitious boundaries should be a minimum from the point of view of the computational realization.

Biisk. Translated from Zhurnal Prikladnoi Mekhaniki i Tekhnicheskoi Fiziki, No. 1, pp. 112-115, January-February, 1988. Original article submitted October 22, 1986.

0021-8944/88/2901-0104$12.50

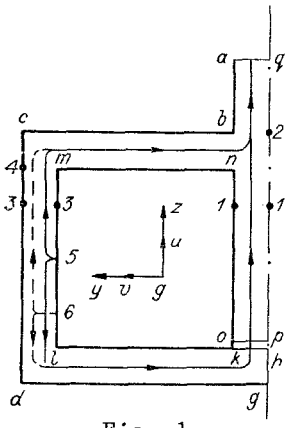

Fig. 1

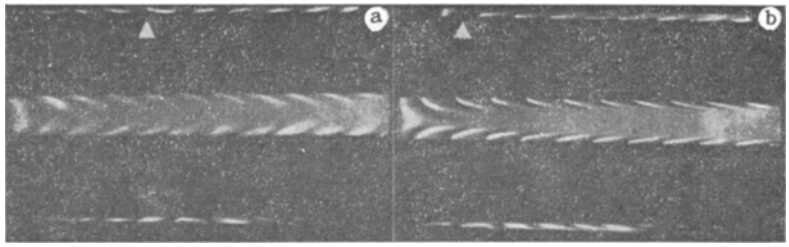

Fig. 2

Thus, the stream function is well-defined everywhere on the contour G, and its values can be obtained by integration: $\Psi = \oint_G y^\nu \rho u dy - y^\nu \rho v dz + c_z$.

The initially unknown integration constant c_Z was sought numerically in the finite-difference iterative process, using one of the following integral expressions:

$$c_z = \int_{y_2}^{y_3} y^\nu \rho u (y, z_1)\, dy; \tag{2.1}$$

$$c_z = -\int_0^{y_1} y^\nu \rho u (y, z_2)\, dy - \int_{z_1}^{z_2} y_1^\nu \rho_0 v_1 dz; \tag{2.2}$$

$$c_z = -\int_{z_1}^{z_2} y_2^\nu \rho_0 v_2 dz + \int_{y_2}^{y_3} y^\nu \rho u (y, z_2)\, dy. \tag{2.3}$$

Here y_1, y_2, y_3, z_1, and z_2 are the coordinates of the sections nk, ℓm, cd, kℓ, and mn of the contour G, respectively; v_1 and v_2 are the linear velocities of injection through the sections nk and ℓm, respectively, and ρ_0 is the density of the injected gas.

If v_1, v_2, and ρ_0 do not depend on the coordinate z, the corresponding integrals on the right-hand sides of Eqs. (2.2) and (2.3) are easy to find, and the remaining integrals were determined numerically from the computational fields of the velocity and density for each iteration. The value of c_Z for subsequent iterations was obtained as an arithmetic mean of the three values of c_Z determined from Eqs. (2.1)-(2.3). As the solution of Eq. (1.1) is convergent, c_Z approaches a constant value which is distinctive for the considered solution only. For the first iteration $c_Z = 0$.

To assign Ψ on the contour G, it is necessary to known the velocity profile on the fictitious boundaries. According to preceding results, the velocity profile for the assumed position of the fictitious boundaries (see Fig. 1) was chosen as $u_f = (2^\nu c_Z/\rho y_1^{\nu+1}) e^\varepsilon (1 - e^{1-\varepsilon})$, where $\varepsilon = (y/y_1)^{\nu+1}$.

3. The experimental study of parallel flows of air in doubly connected domains similar to the domain D revealed a characteristic feature for such flows, namely, the flow

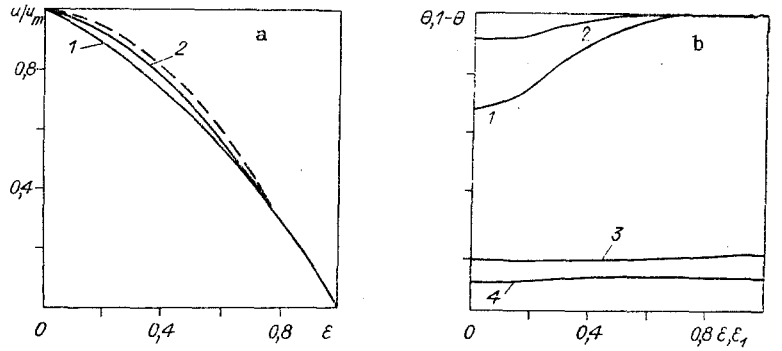

Fig. 3

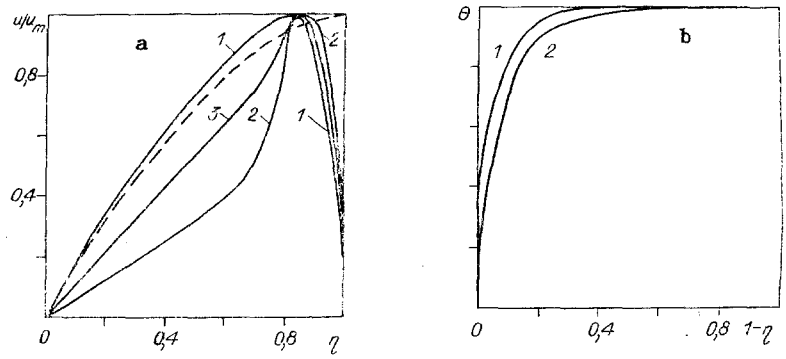

Fig. 4

of gas in the opposite directions from the separation line. The position of the separation line depends on the ratio $v_2/v_1 = \lambda$ and on geometrical parameters of the domain.

The experiments were performed jointly with the Laboratory of Gas Dynamics at the Institute for Thermophysics of the Siberian Branch, Academy of Sciences of the USSR (SO AN SSSR.) To visualize the flow, a 0.2-mm-thick, electrically heated nichrome wire was placed along the porous surface. The gas heated in the wake of the wire was observed with a Toepler instrument (Schlieren method). The comparison between the experimental data and the computational results shows satisfactory agreement for a broad range of λ and geometries of the flow domain. The triangles in Fig. 2a, b show the calculated position of the separation line for $\lambda = 1.17$ and $\gamma = 0.43$, and for $\lambda = 0.48$ and $\gamma = 0.43$, respectively ($\gamma = (y_3 - y_2)/y_1$).

Some results of the numerical study for the axisymmetric flow are shown in Figs. 3a, b and 4a, b. The calculated profiles of the velocity in the cross section 1–1 (see Fig. 1) of the cylindrical channel are shown in Fig. 3a. Profiles 1 and 2 correspond to the velocity for $\Theta_w = \Theta_t = 1$, and $\Theta_w = 0.18$ and $\Theta_t = 0.36$, respectively; u_m is the maximum value of the velocity in this section. The calculated velocity profiles follow closely the analytical solution for channels with injection of the inviscid gas: $u = u_m \cos(\pi/2 \cdot \varepsilon)$ [4]. They are shown by the dashed line in Fig. 3a.

The distribution of the temperature calculated for the same section (curves 1 and 2 for $\Theta_w = 0.18$ and $\Theta_t = 0.36$ respectively), and for the cross section b–2 (curves 3 and 4 for $\Theta_w = 0.45$ and $\Theta_t = 0.36$ respectively) are shown in Fig. 3b for different temperature boundary conditions. Lines 3 and 4 show the dependence of the difference $\theta - 1$ on $\varepsilon_1 = (y/y_b)^2$, where y_b is the radial coordinate of the point b. Clearly, under the assumed boundary conditions, the integral average temperature of the stream in the outlet (cross section b–2) is 10-20% less than the temperature for the velocity profiles in the cylindrical channel. It should be mentioned that the influence of the temperature boundary conditions on the velocity profiles in the cylindrical channel is insignificant.

The velocity profiles calculated for the cross section 3–3 of the annular channel are shown in Fig. 4a. For the isothermal flow, for $\eta = (y^2 - y_2^2)/(y_3^2 - y_2^2) < 0.8$, the velocity profile (line 1) agrees satisfactorily with the analytical solution [4], $u = u_m \sin(\pi/2 \cdot \eta)$ (dashed line). While altering the boundary conditions (curve 2 for $\Theta_w = 0.18$ and $\Theta_t = 0.36$, and curve 3 for $\Theta_w = 0.45$ and $\Theta_t = 0.36$), the velocity profiles in the annular channel deform noticeably. The temperature distribution in the outlet from the annular channel (cross

section 4–m) is shown in Fig. 4b (line 1 for $\Theta = 0.36$ and line 2 for $\Theta = 0.18$). The location of the separation line for $\Theta_w = 0.18$, $\Theta_t = 0.36$, and $\lambda = 1$ is denoted by 5 in Fig. 1 (the solid line shows the direction of the flow), and for $\Theta_w = 0.18$, $\Theta_t = 0.36$, and $\lambda = 2.16$ by 6 (the dashed line shows the direction of the flow). The influence of the flow nonisothermicity on the position of the separation line is not essential.

The numerical experiment conducted to determine the effect of the distance between the fictitious boundaries on the flow pattern showed that, while this distance decreases by δ, the separation line is displaced by approximately $\delta/2$ in the direction which provides better agreement with the experimental data. The influence of the position of the fictitious boundaries on the calculated position of the separation line was also examined. It was established that the calculated position of the separation line is not affected by changes of the position of the fictitious boundaries where the proper velocity profile was assigned. The position of the fictitious boundaries, chosen as hk and op in Fig. 1, seems to be more suitable for investigating the influence of nonisothermicity on the flow pattern, and more convenient from the point of view of numerical realization.

LITERATURE CITED

1. Sh. Smagylov and M. K. Orukhanov, "An approximate method of solving the equations of hydromechanics in multiply connected domains," Dokl. Akad. Nauk SSSR, 260, No. 5, (1981).
2. A. D. Gosman, W. M. Pen, A. K. Runchel, D. B. Spalding, and M. Wolfstein, Heat and Mass Transfer in Recirculating Flows, Academic Press, London (1969).
3. P. J. Roache, Computational Fluid Dynamics, Hermosa Publishers, Alburquerque, New Mexico (1976).
4. A. S. Berman, "Laminar flow in an annulus with porous walls," J. Appl. Phys., 29, No. 1 (1958).

ACOUSTIC PROPERTIES OF A POROUS LAMINATED MEDIUM

M. G. Markov and A. Yu. Yumatov

UDC 624.131

Study of the propagation of elastic waves in nonuniform, saturated, porous media is of interest both theoretically and from the viewpoint of applications in engineering and geophysics. The propagation of elastic waves in such media can be systematically described within the framework of the Frenkel–Biot theory [1-4]. Ignoring thermoelastic effects, we can write the equations of this theory in the form

$$\rho_{11}\frac{\partial^2 u_i}{\partial t^2} + \rho_{12}\frac{\partial^2 v_i}{\partial t^2} = b\frac{\partial}{\partial t}(v_i - u_i) - \frac{\partial P_{ij}}{\partial x_j}, \qquad (1)$$

$$\rho_{12}\frac{\partial^2 u_i}{\partial t^2} + \rho_{22}\frac{\partial^2 v_i}{\partial t^2} = b\frac{\partial}{\partial t}(u_i - v_i) - \frac{\partial s}{\partial x_i},$$

where u_i and v_i are components of the displacement vectors of the skeleton and fluid; ρ_{11} is the effective density of the skeleton moving in the filler; ρ_{22} is the effective density of the filler moving in the porous medium; $\rho_{12} < 0$ is the added density of the fluid; $P_{ij} = Ae\delta_{ij} + 2Ne_{ij} + Q\varepsilon\delta_{ij}$; $s = Qe + R\varepsilon$; $e = \mathrm{div}\mathbf{u}$; $\varepsilon = \mathrm{div}\mathbf{v}$; $e_{ij} = (1/2)(\partial u_i/\partial x_j + \partial u_j/\partial x_i)$; A, N, Q, R are constants of the elastic constraints of the porous medium; the coefficient b characterizes friction due to the motion of the fluid: $b = \mu\Phi^2/K_{pr}$ (μ is the viscosity of the fluid, Φ is bulk porosity, and K_{pr} is the permeability).

After we introduce the two scalar potentials φ_1 and φ_2 of the longitudinal waves and the vector potential of the transverse wave by means of the relations

$$\mathbf{u} = \nabla\varphi_1 + \nabla\varphi_2 + \mathrm{rot}\Psi; \qquad (2)$$

$$\mathbf{v} = M_1\nabla\varphi_1 + M_2\nabla\varphi_2 + M_t\mathrm{rot}\Psi \qquad (3)$$

in the case of harmonic waves, system (1) reduces to a system of two scalar Helmholtz equations

Kalinin. Translated from Zhurnal Prikladnoi Mekhaniki i Tekhnicheskoi Fiziki, No. 1, pp. 115-119, January-February, 1988. Original article submitted June 4, 1986.